

ON DATA-DRIVEN PARAMETERIZATIONS OF MULTIDIMENSIONAL GENERALIZED LANGEVIN DYNAMICS IN THE PRESENCE OF A QUADRATIC POTENTIAL

M. BRAUN*, M. HANKE†, AND N. WOLF‡

Abstract. We propose a numerical algorithm to construct a Markov model with an extended list of variables to parameterize the equation of motion of a multidimensional coarse-grained physical system in an external potential, when memory effects are relevant. Our method uses autocorrelation data of the stationary velocities, but it avoids the inverse problem of finding the corresponding memory kernel from these data in a first step. Rather, the data are used to construct a Prony series approximation of the autocorrelation function, and the parameters of this Prony series provide the corresponding Markov model. Numerical results for molecular dynamics data show a good match for parameterized models with five auxiliary variables for a one-dimensional, and twelve auxiliary variables for a two-dimensional system.

Key words. coarse-graining, stationary process, external potential, extended Markov model

AMS subject classifications. 65L09, 65D15, 41A20

1. Introduction. The generalized Langevin equation is often used in statistical physics as the equation of motion of a particle, or a set of particles, when the background of the system is eliminated from the physical description. Collecting the spatial coordinates of the centers of mass of the particle(s) of interest and their velocities in d -dimensional vectors R and V , respectively, these equations take the form

$$\begin{aligned} \dot{R}(t) &= V(t), \\ M \dot{V}(t) &= -\nabla\Phi(R) - \int_0^t \gamma(t-s)V(s) ds + F(t), \end{aligned} \quad (1.1)$$

together with initial conditions at time $t = 0$. Here, $M \in \mathbb{R}^{d \times d}$ is the (symmetric positive definite) mass matrix, $\Phi = \Phi(R)$ is an external scalar potential, and the memory kernel γ with values in $\mathbb{R}^{d \times d}$ and the (stochastic) fluctuating force vector $F \in \mathbb{R}^d$ represent the interactions of the particle(s) with the eliminated background of the system; this relationship is often associated with a so-called fluctuation-dissipation relation, which couples the autocorrelation function of the fluctuating force and the memory kernel via

$$C_F(t) = \mathbb{E}[F(s+t)F(s)^T] = \frac{1}{\beta} \gamma(t), \quad s, t \geq 0, \quad (1.2)$$

where the constant $\beta > 0$ denotes the inverse temperature. We refer to Zwanzig [31] for the physical reasoning behind this model and to Pavliotis [24] for a discussion of (1.1), (1.2) from a mathematical point of view.

In practice, however, an explicit expression for the memory kernel γ is usually not available, and the same may be true for the external potential. A natural way out of

*Institut für Mathematik, Johannes Gutenberg-Universität Mainz, 55099 Mainz, Germany (bmaximi@uni-mainz.de)

†Institut für Mathematik, Johannes Gutenberg-Universität Mainz, 55099 Mainz, Germany (hanke@math.uni-mainz.de)

‡Institut für Chemie, Technische Universität Darmstadt, 64287 Darmstadt, Germany (wolf@cpc.tu-darmstadt.de)

the latter problem is to linearize the generalized Langevin equation and to replace Φ by a quadratic potential

$$\Phi(x) = \frac{1}{2} x^T \Omega x, \quad x \in \mathbb{R}^d, \quad (1.3)$$

where the symmetric positive definite stiffness matrix Ω is deduced from the sample covariance of the particle positions; cf., e.g., Ma, Li, and Liu [22], and Remark 2.2 below.

As far as the memory kernel is concerned, we first note that it is quite common in computational physics to introduce a set of auxiliary variables Z in order to replace the non-Markovian generalized Langevin equation (1.1) by a Markovian model

$$\begin{aligned} \dot{X}(t) &= Y(t), \\ d \begin{bmatrix} Y \\ Z \end{bmatrix} &= \begin{bmatrix} -M^{-1} \nabla \Phi(X) \\ 0 \end{bmatrix} + \begin{bmatrix} 0 & B^T \\ -C & A \end{bmatrix} \begin{bmatrix} Y \\ Z \end{bmatrix} dt + \begin{bmatrix} 0 \\ L \end{bmatrix} dW, \end{aligned} \quad (1.4)$$

with constant matrices A , B , C , and L , where W is a d -dimensional Brownian motion, and X and Y stand for approximations of R and V , respectively. Note that this approximation is exact, if

$$\gamma(t) = M B^T e^{tA} C, \quad t \geq 0; \quad (1.5)$$

compare [24, Proposition 8.1] or (3.16) below. Accordingly, the standard approach in the physics literature (cf., e.g., [12, 18, 19]) to find suitable parameters for (1.4) is a two-step procedure, which consists in (i) fitting the memory kernel γ to observation data – usually correlation data of V and $\nabla \Phi(X)$ –, and (ii) subsequently approximating γ by an exponential model of the form (1.5). See also [17] for a conceptually different approach.

Note that under the assumption that Φ is given by (1.3), the system (1.4) can be rewritten as an Ornstein-Uhlenbeck system

$$d \begin{bmatrix} Y \\ Z \\ X \end{bmatrix} = \begin{bmatrix} 0 & B^T & -M^{-1} \Omega \\ -C & A & 0 \\ I & 0 & 0 \end{bmatrix} \begin{bmatrix} Y \\ Z \\ X \end{bmatrix} dt + \begin{bmatrix} 0 \\ L \\ 0 \end{bmatrix} dW \quad (1.6)$$

of dimension $N > 2d$. Our contribution in this paper is an extension of a method presented earlier in [5, 13] to directly construct a system of the form (1.6) from a finite number of equidistant samples of the velocity autocorrelation function only; our method does not even need the stiffness matrix Ω as input, in which case the (1,3)-block of the coefficient matrix in (1.6) will merely be an approximation of $-M^{-1} \Omega$. We mention that there exist similarities to a method employed by Baczewski and Bond [3], and we will briefly elaborate on this in Remark 3.1.

The outline of this paper is as follows. In the next section we discuss the existence of stationary solutions of the generalized Langevin system (1.1), and we derive some properties of the associated autocorrelation functions. Subsequently, in Section 3, we present the modifications of the method in [5, 13] which are necessary to obtain an Ornstein-Uhlenbeck system in the form (1.6); as we will see, by a proper post-processing of our system we automatically recover the approximation X of R from the auxiliary variables. Section 4 reviews the numerical ingredients of the implementation of our method. Here we aim for a self-contained presentation, but we omit technical

details which have already been described in previous work. In Subsection 4.4 we also briefly comment on the case that position autocorrelation data instead of velocity autocorrelation data are given; in principle it is easy to modify our algorithm accordingly, but our numerical results have been somewhat inferior for this modification. Finally, Section 5 presents numerical examples using molecular dynamics simulation data for one, respectively two, trapped particles as input.

2. Stationary solutions of the generalized Langevin equation. In this section we derive sufficient conditions for the existence of a stationary solution (R, V) of the generalized Langevin equation (1.1), (1.2), in the presence of a quadratic potential (1.3). Without loss of generality we assume throughout that the mass matrix in (1.1) is of the form

$$M = mI \tag{2.1}$$

for some scalar mass value $m > 0$; otherwise we reformulate (1.1) as a generalized Langevin equation for $M^{-1/2}R$ and $M^{-1/2}V$. We will further assume that γ is extended to all of \mathbb{R} by

$$\gamma(t) = \gamma(-t)^T, \quad t < 0,$$

and that this function is absolutely integrable and of strictly positive type, i.e., its Fourier transform

$$\widehat{\gamma}(\omega) = \int_{-\infty}^{\infty} e^{-i\omega t} \gamma(t) dt$$

is positive definite for all $\omega \in \mathbb{R}$. Note that this guarantees the existence of the fluctuating force term in (1.1), i.e., a centered stationary Gaussian process F which satisfies (1.2) for all $s, t \in \mathbb{R}$; compare, e.g., Lindgren [21].

PROPOSITION 2.1. *Let $\gamma \in L^1(\mathbb{R})$ be a function of strictly positive type with values in $\mathbb{R}^{d \times d}$, and let the fluctuating force F be a centered stationary Gaussian process satisfying (1.2). Then the generalized Langevin equation (1.1) with mass matrix (2.1) and initial data*

$$\begin{bmatrix} R(0) \\ V(0) \end{bmatrix} \sim \mathcal{N}(0, \Sigma) \quad \text{with} \quad \Sigma = \frac{1}{\beta m} \begin{bmatrix} m\Omega^{-1} & 0 \\ 0 & I \end{bmatrix} \tag{2.2}$$

has a unique solution (R, V) , and this solution is a centered stationary Gaussian process, provided the initial data are independent of the fluctuating force. The autocorrelation function of this solution is given by

$$C(t) = r(t)\Sigma, \quad t \geq 0, \tag{2.3}$$

where $r : \mathbb{R}_0^+ \rightarrow \mathbb{R}^{2d \times 2d}$ solves the Volterra integrodifferential equation

$$r'(t) = - \begin{bmatrix} 0 & -I \\ \Omega/m & 0 \end{bmatrix} r(t) - \int_0^t \begin{bmatrix} 0 & 0 \\ 0 & \gamma(t-s)/m \end{bmatrix} r(s) ds, \quad r(0) = I. \tag{2.4}$$

Proof. Let

$$U = \begin{bmatrix} R \\ V \end{bmatrix}, \quad \Gamma = \begin{bmatrix} 0 & 0 \\ 0 & \gamma/m \end{bmatrix}, \quad \text{and} \quad D = \begin{bmatrix} 0 & -I \\ \Omega/m & 0 \end{bmatrix}, \tag{2.5}$$

so that the system (1.1) can be rewritten in the form

$$\dot{U} = -DU(t) - \int_0^t \Gamma(t-s)U(s) ds + \tilde{F}(t),$$

where

$$\tilde{F}(t) = \begin{bmatrix} 0 \\ F(t)/m \end{bmatrix}.$$

According to (1.2) \tilde{F} is a centered stationary Gaussian process with autocorrelation function

$$C_{\tilde{F}}(t) = \frac{1}{\beta m} \Gamma(t) = \Gamma(t)\Sigma, \quad t \geq 0, \quad (2.6)$$

with the second identity following readily from the definitions of Γ and Σ .

The assertion of the proposition is now an immediate consequence of the theory developed in [14]: Since

$$D\Sigma + \Sigma D^T = 0,$$

the claim follows from [14, Theorem 2.3] by virtue of (2.6). \square

REMARK 2.2. It follows from (2.2) that

$$\Omega = \frac{1}{\beta} \mathbb{E}[R(t)R(t)^T]^{-1} = \frac{1}{\beta} C_R(0)^{-1}, \quad t \geq 0.$$

Hence, this provides a means to recover Ω from the position autocorrelation function. \diamond

Rewriting

$$r = \begin{bmatrix} r_{11} & r_{12} \\ r_{21} & r_{22} \end{bmatrix} \quad (2.7)$$

in terms of four $d \times d$ matrix blocks, the integro-differential equation (2.4) becomes

$$\begin{aligned} r'_{11}(t) &= r_{21}(t), & r_{11}(0) &= I, \\ r'_{12}(t) &= r_{22}(t), & r_{12}(0) &= 0, \\ m r'_{21}(t) &= -\Omega r_{11}(t) - \int_0^t \gamma(t-s)r_{21}(s) ds, & r_{21}(0) &= 0, \\ m r'_{22}(t) &= -\Omega r_{12}(t) - \int_0^t \gamma(t-s)r_{22}(s) ds, & r_{22}(0) &= I. \end{aligned} \quad (2.8)$$

From this one can derive the following properties of C_V .

THEOREM 2.3. *Under the assumptions of Proposition 2.1 let (R, V) be the corresponding stationary solution of (1.1). Then the autocorrelation function C_V of the velocity component of this solution is differentiable at $t = 0$ with*

$$C'_V(0) = 0, \quad (2.9)$$

and it is absolutely integrable with

$$\int_0^\infty C_V(t) dt = 0. \quad (2.10)$$

Furthermore, if in addition

$$\int_0^\infty t |\gamma(t)| dt < \infty, \quad (2.11)$$

then

$$\int_0^\infty t C_V(t) dt = -\frac{1}{\beta} \Omega^{-1}. \quad (2.12)$$

Proof. According to (2.3), (2.4), (2.2), and (2.7) the autocorrelation function of the V -component of the stationary solution of (1.1) is given by

$$C_V(t) = \frac{1}{\beta m} r_{22}(t) \quad \text{for } t \geq 0.$$

By virtue of (2.8) this implies that C_V is differentiable for $t > 0$, and the right-sided differential quotient of C_V at $t = 0$ is given by

$$C'_V(0+) = \lim_{\substack{t \rightarrow 0 \\ t > 0}} \frac{C_V(t) - C_V(0)}{t} = \frac{1}{\beta m} r'_{22}(0) = -\frac{1}{\beta m^2} \Omega r_{12}(0) = 0.$$

Further, since $C_V(-t) = C_V(t)^T$ for $t > 0$, the left-sided difference quotient $C'_V(0-)$ has the same value. This proves the first claim.

Concerning the integral of C_V we first need to settle that $C_V \in L^1(\mathbb{R}^+)$. To this end we investigate the matrices

$$H(\zeta) = \zeta I + D + \mathcal{L}\Gamma(\zeta) \quad (2.13)$$

for $\zeta \in \mathbb{C}$ with $\operatorname{Re} \zeta \geq 0$; in (2.13) the matrices Γ and D are taken from (2.5), and

$$\mathcal{L}\Gamma(\zeta) = \int_0^\infty e^{-\zeta t} \Gamma(t) dt$$

denotes the Laplace transform of Γ , which is well defined for $\operatorname{Re} \zeta \geq 0$, because $\Gamma \in L^1(\mathbb{R}^+)$. Let $x, y \in \mathbb{C}^d$ be such that

$$H(\zeta_0) \begin{bmatrix} x \\ y \end{bmatrix} = \begin{bmatrix} \zeta_0 I & -I \\ \Omega/m & \zeta_0 I + \mathcal{L}\gamma(\zeta_0)/m \end{bmatrix} \begin{bmatrix} x \\ y \end{bmatrix} = \begin{bmatrix} 0 \\ 0 \end{bmatrix} \quad (2.14)$$

for any given ζ_0 with $\operatorname{Re} \zeta_0 \geq 0$. Then the scalar complex-valued function

$$f(\zeta) := \frac{1}{\beta} \begin{bmatrix} x \\ y \end{bmatrix}^* \Sigma^{-1} H(\zeta) \begin{bmatrix} x \\ y \end{bmatrix} = \begin{bmatrix} x \\ y \end{bmatrix}^* \begin{bmatrix} \zeta \Omega & -\Omega \\ \Omega & m\zeta I + \mathcal{L}\gamma(\zeta) \end{bmatrix} \begin{bmatrix} x \\ y \end{bmatrix},$$

which is analytic in the open right complex half plane, vanishes for $\zeta = \zeta_0$; furthermore, on the imaginary axis, i.e., for $\zeta = i\omega$ with $\omega \in \mathbb{R}$, its real part is given by

$$\begin{aligned} \operatorname{Re} f(i\omega) &= \frac{1}{2\beta} \begin{bmatrix} x \\ y \end{bmatrix}^* \left(\Sigma^{-1} H(i\omega) + (\Sigma^{-1} H(i\omega))^* \right) \begin{bmatrix} x \\ y \end{bmatrix} \\ &= \frac{1}{2} \begin{bmatrix} x \\ y \end{bmatrix}^* \begin{bmatrix} 0 & 0 \\ 0 & \mathcal{L}\gamma(i\omega) + (\mathcal{L}\gamma(i\omega))^* \end{bmatrix} \begin{bmatrix} x \\ y \end{bmatrix} = \frac{1}{2} y^* \widehat{\gamma}(\omega) y. \end{aligned}$$

Therefore, as γ is assumed to be strictly positive real, the real part of f is either zero on the entire imaginary axis when $y = 0$, or it is positive on the entire imaginary axis when $y \neq 0$. Since $\operatorname{Re} f$ is a harmonic function on the right half plane, it follows from the maximum principle that in the latter case $\operatorname{Re} f$ is positive in the entire right half plane; accordingly, $f(\zeta_0) = 0$ implies that $y = 0$.

Inserting this into (2.14) we see that

$$\begin{bmatrix} 0 \\ 0 \end{bmatrix} = H(\zeta_0) \begin{bmatrix} x \\ y \end{bmatrix} = \begin{bmatrix} \zeta_0 x \\ \Omega x/m \end{bmatrix},$$

which shows that $x = 0$, too, because Ω is nonsingular. In other words, the null space of $H(\zeta_0)$ is trivial, and we therefore have established that $H(\zeta)$ is nonsingular for every ζ in the closed right half plane. Now it is known (compare Gripenberg, London, and Staffans [10, Theorem 3.3.5]) that this is equivalent to the fact that the (unique) solution r of (2.4) belongs to $L^1(\mathbb{R}^+)$, and so does r' . From this it readily follows that $r(t) \rightarrow 0$ as $t \rightarrow \infty$. We thus have shown that $C_V \in L^1(\mathbb{R}^+)$, and (2.8) implies that

$$\int_0^\infty C_V(t) dt = \frac{1}{\beta m} \int_0^\infty r_{22}(t) dt = \frac{1}{\beta m} r_{12}(t) \Big|_{t=0}^\infty = 0. \quad (2.15)$$

If γ also satisfies the decay condition (2.11) then [10, Theorem 4.4.13] implies that the same decay condition is true for r and r' , and hence, $tr(t) \rightarrow 0$ as $t \rightarrow \infty$. We therefore obtain by partial integration that

$$\begin{aligned} \int_0^\infty t C_V(t) dt &= \frac{1}{\beta m} \int_0^\infty t r_{22}(t) dt = \frac{1}{\beta m} t r_{12}(t) \Big|_{t=0}^\infty - \frac{1}{\beta m} \int_0^\infty r_{12}(t) dt \\ &= -\frac{1}{\beta m} \int_0^\infty r_{12}(t) dt. \end{aligned}$$

It further follows from (2.8) that

$$r_{12}(t) = -\Omega^{-1} \left(m r'_{22}(t) + \int_0^t \gamma(t-s) r_{22}(s) ds \right),$$

and inserting this into the previous identity yields

$$\begin{aligned} \int_0^\infty t C_V(t) dt &= \frac{1}{\beta m} \Omega^{-1} \left(\int_0^\infty m r'_{22}(t) dt + \int_0^\infty \int_0^t \gamma(t-s) r_{22}(s) ds dt \right) \\ &= \frac{1}{\beta m} \Omega^{-1} \left(m r_{22}(t) \Big|_{t=0}^\infty + \int_0^\infty \gamma(\tau) d\tau \int_0^\infty r_{22}(s) ds \right). \end{aligned}$$

According to (2.15) the integral over r_{22} vanishes, and hence, under the given assumptions, we arrive at

$$\int_0^\infty t C_V(t) dt = -\frac{1}{\beta} \Omega^{-1} r_{22}(0) = -\frac{1}{\beta} \Omega^{-1}$$

by virtue of (2.8) again. \square

REMARK 2.4. In statistical physics the integral over C_V is known as the self-diffusion coefficient of the macroparticle, cf., e.g., [31]. This coefficient being equal to zero according to (2.10) reflects the fact that the position of the macroparticle is a centered stationary process. \diamond

3. A Markov approximation. Theorem 2.3 implies that the autocorrelation function of the velocity component of the stationary solution of (1.1) carries the entire information about the quadratic potential. Let us accordingly assume that finitely many equidistant samples $C_V(\nu\tau)$, $\nu = 0, \dots, n$, of the autocorrelation function are given for some $\tau > 0$ and $n \in \mathbb{N}$; as stated in the introduction our goal is to set up an Ornstein-Uhlenbeck equation

$$d \begin{bmatrix} Y \\ Z \\ X \end{bmatrix} = \begin{bmatrix} 0 & B^T & -\Omega_0/m \\ -C & A & 0 \\ I & 0 & 0 \end{bmatrix} \begin{bmatrix} Y \\ Z \\ X \end{bmatrix} dt + \begin{bmatrix} 0 \\ L \\ 0 \end{bmatrix} dW \quad (3.1)$$

of dimension $N > 2d$ with auxiliary variables $Z \in \mathbb{R}^{N-2d}$ and $\Omega_0 \approx \Omega$, such that the components $Y \in \mathbb{R}^d$ and $X \in \mathbb{R}^d$ of its stationary solution satisfy $Y \approx V$ and $X \approx R$ in the sense that their correlations are in good agreement.

To this end we employ the method developed in [13] for scalar stochastic processes and extended in [5] to the case of vector-valued processes; this method will be briefly reviewed in Section 4. It is designed to provide an Ornstein-Uhlenbeck system

$$d \begin{bmatrix} Y \\ Z_0 \end{bmatrix} = \begin{bmatrix} 0 & B_0^T \\ -C_0 & A_0 \end{bmatrix} \begin{bmatrix} Y \\ Z_0 \end{bmatrix} dt + \begin{bmatrix} 0 \\ L_0 \end{bmatrix} dW \quad (3.2)$$

of dimension N with auxiliary variables $Z_0 \in \mathbb{R}^{N-d}$. The real drift matrix of (3.2), denoted by A in the sequel, is chosen to be stable, i.e., its eigenvalues belong to

$$\mathbb{C}^- = \{ \lambda \in \mathbb{C} : \text{Re } \lambda < 0 \},$$

and the matrix $L_0 \in \mathbb{R}^{(N-d) \times d}$ is constructed in such a way that the (unique) stationary solution of (3.2) satisfies

$$C_Y(0) = \mathbb{E}[Y(0)Y(0)^T] = C_V(0) = \frac{1}{\beta m} I \quad \text{and} \quad \mathbb{E}[Y(0)Z_0(0)^T] = 0. \quad (3.3)$$

REMARK 3.1. We recall that the system (3.2) can be recast as a generalized Langevin equation

$$Y'(t) = - \int_0^t \gamma_{\text{eff}}(t-s)Y(s) ds + F_{\text{eff}}(t)$$

for Y with an effective memory kernel γ_{eff} and associated fluctuating force F_{eff} , which comes without any external potential. The idea of using an effective equation of this sort for $Y \approx V$, when Φ in (1.1) is given by (1.3), has been the starting point of the construction of Baczewski and Bond in [3]; they employ the Laplace transform to connect the effective memory kernel to the given velocity autocorrelation function C_V . The advantage of our approach is that it avoids the (ill-posed) inverse Laplace transform and determines suitable parameters for (3.2) directly from the data. \diamond

The $d \times d$ zero block in the upper left corner of the drift matrix A in (3.2) is a consequence of the side condition

$$C_Y'(0) = 0, \quad (3.4)$$

which is imposed in [5, 13] to mimic (2.9). In contrast to the method as it is presented in [5, 13], here we further impose the additional constraint

$$\int_0^\infty C_Y(t) dt = 0 \quad (3.5)$$

because of (2.10); see Section 4 for details. From (3.2) and (3.3) it follows that

$$C_Y(t) = \frac{1}{\beta m} E^T e^{tA} E \quad \text{with} \quad E = \begin{bmatrix} I \\ 0 \end{bmatrix} \quad (3.6)$$

for $t \geq 0$, cf., e.g., [24, Section 3.7], and hence, (3.4) and (3.5) are equivalent to

$$E^T A E = 0 \quad \text{and} \quad E^T A^{-1} E = 0, \quad (3.7)$$

respectively.

Since $C_Y(t) = C_Y(-t)^T$ for $t < 0$, (3.6) implies that the Fourier transform of C_Y is given by

$$\begin{aligned} \widehat{C}_Y(\omega) &= \frac{1}{\beta m} \int_{-\infty}^0 e^{-i\omega t} E^T e^{-tA^T} E dt + \frac{1}{\beta m} \int_0^{\infty} e^{-i\omega t} E^T e^{tA} E dt \\ &= \frac{1}{\beta m} (\kappa(i\omega)^* + \kappa(i\omega)), \end{aligned} \quad (3.8)$$

where

$$\kappa(\zeta) = E^T (\zeta I - A)^{-1} E \quad (3.9)$$

is the so-called transfer function of the system (3.2). This is a real rational function, i.e., $\kappa(\bar{z}) = \overline{\kappa(z)}$ for all $z \in \mathbb{C}$, which is analytic in a neighborhood of the closed right half-plane because A is a stable matrix. Further, since every autocorrelation function is a function of positive type, cf., e.g., [24, Lemma 1.2], it follows from (3.8) that the Hermitian part of $\kappa(\zeta)$ is positive semidefinite for every ζ on the imaginary axis. In system theory a function κ with these properties is said to be positive real; compare Anderson and Vongpanitlerd [2].

THEOREM 3.2. *Let the drift matrix A of (3.2) be stable, and let (3.2) have a stationary solution which satisfies (3.3). Assume further that $E^T A^{-1} E = 0$ with E as in (3.6). Then the matrix block A_0 in (3.2) has a d -dimensional null space $\mathcal{N}(A_0)$, and this is a complementary subspace of the range space $\mathcal{R}(A_0) \subset \mathbb{R}^{N-d}$.*

Proof. We start by noting that B_0 and C_0 must have full rank, because A is stable, and hence nonsingular. For the same reason the null spaces of A_0 and B_0^T must not have a nontrivial vector z in common, for otherwise $[0; z]$ is a nontrivial element of the null space of A . It follows that the dimension of the null space of A_0 can be at most d , for the null space of B_0^T already has dimension $N - d$.

Consider now any vector

$$w \in \mathcal{R}(A_0) \cap \mathcal{R}(C_0).$$

Then there exist $z \in \mathbb{R}^{N-d}$ and $y \in \mathbb{R}^d$ with

$$w = A_0 z = C_0 y,$$

and hence,

$$A \begin{bmatrix} y \\ z \end{bmatrix} = \begin{bmatrix} 0 & B_0^T \\ -C_0 & A_0 \end{bmatrix} \begin{bmatrix} y \\ z \end{bmatrix} = \begin{bmatrix} B_0^T z \\ 0 \end{bmatrix}. \quad (3.10)$$

Due to the assumption that $E^T A^{-1} E = 0$, it follows from (3.10) that

$$0 = E^T A^{-1} E B_0^T z = E^T A^{-1} \begin{bmatrix} B_0^T z \\ 0 \end{bmatrix} = E^T \begin{bmatrix} y \\ z \end{bmatrix} = y,$$

and this in turn implies that $w = C_0 y = 0$. Accordingly, the range spaces of A_0 and C_0 are complementary spaces, and hence, $\mathcal{R}(A_0) \oplus \mathcal{R}(C_0)$ has dimension $(N - d - \dim \mathcal{N}(A_0)) + d$. Since this cannot be larger than $N - d$, we necessarily have $\dim \mathcal{N}(A_0) \geq d$, and therefore the dimension of the null space of A_0 is exactly equal to d .

For the final assertion let us assume that there is some nontrivial element $z \in \mathcal{R}(A_0) \cap \mathcal{N}(A_0)$. Then there exists $x \in \mathbb{R}^{N-d}$, such that

$$A_0 x = z \quad \text{and} \quad A_0 z = 0, \quad (3.11)$$

and since B_0^T is a bijection from $\mathcal{N}(A_0)$ to \mathbb{R}^d there further exists $x' \in \mathcal{N}(A_0)$ with

$$B_0^T x' = B_0^T z.$$

Accordingly,

$$A \begin{bmatrix} 0 \\ x - x' \end{bmatrix} = \begin{bmatrix} 0 & B_0^T \\ -C_0 & A_0 \end{bmatrix} \begin{bmatrix} 0 \\ x - x' \end{bmatrix} = \begin{bmatrix} B_0^T(x - x') \\ A_0 x - A_0 x' \end{bmatrix} = \begin{bmatrix} 0 \\ z \end{bmatrix},$$

and hence,

$$A^2 \begin{bmatrix} 0 \\ x - x' \end{bmatrix} = A \begin{bmatrix} 0 \\ z \end{bmatrix} = \begin{bmatrix} 0 & B_0^T \\ -C_0 & A_0 \end{bmatrix} \begin{bmatrix} 0 \\ z \end{bmatrix} = \begin{bmatrix} B_0^T z \\ A_0 z \end{bmatrix} = \begin{bmatrix} B_0^T z \\ 0 \end{bmatrix}.$$

This shows that for $y = B_0^T z \in \mathbb{R}^d$ there holds

$$y^T E^T A^{-2} E y = y^T E^T A^{-2} \begin{bmatrix} B_0^T z \\ 0 \end{bmatrix} = y^T E^T \begin{bmatrix} 0 \\ x - x' \end{bmatrix} = 0. \quad (3.12)$$

Note that $y \neq 0$ because $z \neq 0$ and the intersection of the null spaces of B_0^T and A_0 is trivial.

As before, let C_Y be the autocorrelation function of the Y -component of the stationary solution of (3.2), and κ be given by (3.9). Since κ is positive real, the scalar rational function

$$f(\zeta) := y^* \kappa(\zeta) y \quad (3.13)$$

with y of (3.12) is analytic in a neighborhood of the closed right-half complex plane with

$$\operatorname{Re} f(i\omega) \geq 0 \quad \text{for every } \omega \in \mathbb{R}.$$

By the maximum principle for harmonic functions, $\operatorname{Re} f$ must therefore be positive in the open right-half plane, for if it has a zero at some ζ_0 with $\operatorname{Re} \zeta_0 > 0$, then $\operatorname{Re} f$ is identically zero, in contradiction to

$$\lim_{\zeta \rightarrow \infty} \zeta f(\zeta) = \|y\|_2^2 > 0.$$

On the other hand, (3.9), (3.7), and (3.12) imply that

$$f(0) = -y^* E^T A^{-1} E y = 0 \quad \text{and} \quad f'(0) = -y^* E^T A^{-2} E y = 0,$$

i.e., f has a multiple zero at $\zeta = 0$. Due to the local behavior of analytic functions, cf., e.g., Ahlfors [1, Section 4.3], this contradicts the fact that its real part is positive

in the intersection of any small neighborhood of $\zeta = 0$ and the open right half-plane. This proves that no nontrivial vector z satisfying (3.11) can exist, and therefore $\mathcal{R}(A_0)$ and $\mathcal{N}(A_0)$ are complementary subspaces. \square

Consider the coordinate transformation which turns A_0 into its real Jordan canonical form. We split accordingly the solution component Z_0 of (3.2) into new variables $Z \in \mathbb{R}^{N-2d}$ corresponding to the nonzero eigenvalues of A_0 (its range space) and the remaining eigencomponents $X_0 \in \mathbb{R}^d$ from the null space of A_0 ; denoting by $A \in \mathbb{R}^{(N-2d) \times (N-2d)}$ the Jordan block associated with the nonzero eigenvalues of A_0 we can thus rewrite (3.2) as

$$d \begin{bmatrix} Y \\ Z \\ X_0 \end{bmatrix} = \begin{bmatrix} 0 & B^T & B_1^T \\ -C & A & 0 \\ -C_1 & 0 & 0 \end{bmatrix} \begin{bmatrix} Y \\ Z \\ X_0 \end{bmatrix} dt + \begin{bmatrix} 0 \\ L \\ L_1 \end{bmatrix} dW.$$

Since the drift matrix of this equation is similar to the matrix A in (3.2), it is also nonsingular, and hence, $C_1 \in \mathbb{R}^{d \times d}$ is nonsingular. Accordingly, introducing $X = -C_1^{-1}X_0$ we obtain the equivalent system

$$d \begin{bmatrix} Y \\ Z \\ X \end{bmatrix} = \begin{bmatrix} 0 & B^T & -\Omega_0/m \\ -C & A & 0 \\ I & 0 & 0 \end{bmatrix} \begin{bmatrix} Y \\ Z \\ X \end{bmatrix} dt + \begin{bmatrix} 0 \\ L \\ L_2 \end{bmatrix} dW \quad (3.14)$$

with

$$\Omega_0 = m B_1^T C_1 \quad \text{and} \quad L_2 = -C_1^{-1} L_1.$$

This is the Langevin equation (3.1) that we have been heading for.

PROPOSITION 3.3. *Under the assumptions of Theorem 3.2 the matrix block Ω_0 in (3.14) is symmetric positive definite and L_2 is equal to zero. Furthermore, (3.14) admits a stationary solution, the covariance matrix of which is given by*

$$\Sigma_0 = \frac{1}{\beta m} \begin{bmatrix} I & 0 & 0 \\ 0 & \Sigma_{22} & 0 \\ 0 & 0 & m\Omega_0^{-1} \end{bmatrix},$$

where the symmetric positive semidefinite matrix block $\Sigma_{22} \in \mathbb{R}^{(N-2d) \times (N-2d)}$ satisfies

$$A\Sigma_{22} + \Sigma_{22}A^T = -\beta m LL^T \quad \text{and} \quad \Sigma_{22}B = C \quad (3.15)$$

with B and C of (3.14).

Proof. We have already seen that under the given assumptions (3.14) admits a stationary solution, whose components $Z(t)$ and $X(t)$ are uncorrelated with $Y(t)$ because of (3.3). Accordingly, the covariance matrix Σ_0 of this stationary solution of (3.14) is given by

$$\Sigma_0 = \frac{1}{\beta m} \begin{bmatrix} I & 0 & 0 \\ 0 & \Sigma_{22} & \Sigma_{23} \\ 0 & \Sigma_{23}^T & \Sigma_{33} \end{bmatrix}$$

for appropriate matrix blocks Σ_{22} , Σ_{23} , Σ_{33} , and the associated Lyapunov equation

for Σ_0 takes the form

$$\begin{aligned} & \begin{bmatrix} 0 & B^T & -\Omega_0/m \\ -C & \Lambda & 0 \\ I & 0 & 0 \end{bmatrix} \begin{bmatrix} I & 0 & 0 \\ 0 & \Sigma_{22} & \Sigma_{23} \\ 0 & \Sigma_{23}^T & \Sigma_{33} \end{bmatrix} + \begin{bmatrix} I & 0 & 0 \\ 0 & \Sigma_{22} & \Sigma_{23} \\ 0 & \Sigma_{23}^T & \Sigma_{33} \end{bmatrix} \begin{bmatrix} 0 & -C^T & I \\ B & \Lambda^T & 0 \\ -\Omega_0^T/m & 0 & 0 \end{bmatrix} \\ & = -\beta m \begin{bmatrix} 0 & 0 & 0 \\ 0 & LL^T & LL_2^T \\ 0 & L_2L^T & L_2L_2^T \end{bmatrix}. \end{aligned}$$

Evaluating the (3,3) block term on the left-hand side of this equation it readily follows that $L_2 = 0$. A subsequent evaluation of the (2,3) block term yields

$$\Lambda \Sigma_{23} = -\beta m LL_2^T = 0,$$

and since Λ is nonsingular, it follows that $\Sigma_{23} = 0$.

To determine Σ_{33} we compute the (3,1) block identity in the Lyapunov equation:

$$I + \Sigma_{23}^T B - \Sigma_{33} \Omega_0^T / m = 0.$$

Since we already know that $\Sigma_{23} = 0$ we conclude that

$$\Sigma_{33} \Omega_0^T = m I.$$

This implies that Σ_{33} and Ω_0 have full rank, and that

$$\Sigma_{33} = m \Omega_0^{-T}.$$

Clearly, Ω_0 must therefore be symmetric and positive definite. Finally, an evaluation of the (2,2) and (2,1) block terms gives the remaining two equations (3.15) for Σ_{22} . \square

The second block equation of (3.14) yields the representation

$$Z(t) = e^{t\Lambda} Z(0) - \int_0^t e^{(t-s)\Lambda} C Y(s) ds + \int_0^t e^{(t-s)\Lambda} L dW(s), \quad t \geq 0,$$

of the auxiliary Z -variables of (3.14). Inserting this expression into the first block equation of (3.14) and making use of Proposition 3.3 we conclude that X and Y satisfy the system of stochastic differential equations

$$\begin{aligned} \dot{X}(t) &= Y(t), \\ m \dot{Y}(t) &= -\Omega_0 X(t) - \int_0^t m B^T e^{(t-s)\Lambda} C Y(s) ds + F_0(t), \end{aligned} \quad (3.16)$$

with

$$F_0(t) = m B^T e^{t\Lambda} Z(0) + \int_0^t m B^T e^{(t-s)\Lambda} L dW(s).$$

This system has the same structure as the original model (1.1) that we have started with, and the memory kernel γ_0 associated with (3.16) has the form

$$\gamma_0(t) = m B^T e^{t\Lambda} C, \quad t \geq 0,$$

which is absolutely integrable whenever Λ is a stable matrix; see Remark 3.4 below. It can further be shown (compare, e.g., the computation in [24, Section 8.2]) that

in this case the fluctuating force F_0 is a centered stationary Gaussian process with autocorrelation function

$$C_{F_0}(t) = \mathbb{E}[F_0(s+t)F_0(s)^T] = \frac{1}{\beta} \gamma_0(t), \quad t \geq 0,$$

provided that

$$Z(0) \sim \mathcal{N}\left(0, \frac{1}{\beta m} \Sigma_{22}\right),$$

independent of the Brownian motion W . This should be compared to (1.2).

REMARK 3.4. Recall that the autocorrelation function C_Y of the Y -component of the stationary solution of (3.14) is a function of positive type, but beware of the fact that it fails to be of strictly positive type under the assumptions of Theorem 3.2 because $\widehat{C}_Y(0) = 0$ by virtue of (3.5).

In this situation a sufficient condition for A to be stable is that $\widehat{C}_Y(\omega)$ is positive definite for every $\omega \neq 0$. A simple argument for this statement is as follows. Assume that A has a nonzero eigenvalue λ on the imaginary axis or in the open right half-plane. Let $z \in \mathbb{C}^{N-d}$ be an associated eigenvector of A_0 , and denote the coefficient matrix of (3.2) once again by A . Then $B_0^T z$ must be different from zero, for otherwise

$$A \begin{bmatrix} 0 \\ z \end{bmatrix} = \begin{bmatrix} 0 & B_0^T \\ -C_0 & A_0 \end{bmatrix} \begin{bmatrix} 0 \\ z \end{bmatrix} = \begin{bmatrix} B_0^T z \\ A_0 z \end{bmatrix} = \begin{bmatrix} 0 \\ \lambda z \end{bmatrix},$$

and hence, λ also belongs to the spectrum of A ; since A is stable, this is not possible. Accordingly,

$$(\lambda I - A) \begin{bmatrix} 0 \\ z \end{bmatrix} = \begin{bmatrix} \lambda I & -B_0^T \\ C_0 & \lambda I - A_0 \end{bmatrix} \begin{bmatrix} 0 \\ z \end{bmatrix} = \begin{bmatrix} -B_0^T z \\ 0 \end{bmatrix},$$

and hence, for $y = -B_0^T z \neq 0$ it follows that

$$y^* E^T (\lambda I - A)^{-1} E y = y^* E^T (\lambda I - A)^{-1} \begin{bmatrix} -B_0^T z \\ 0 \end{bmatrix} = y^* E^T \begin{bmatrix} 0 \\ z \end{bmatrix} = 0.$$

This means that the rational function f defined in (3.13) vanishes at $\zeta = \lambda$. As discussed in the proof of Theorem 3.2, however, this rational function cannot have roots in the open right-half plane, and it can neither have a root $\zeta = i\omega \neq 0$ on the imaginary axis because

$$2 \operatorname{Re} f(i\omega) = \beta m y^* \widehat{C}_Y(\omega) y \quad \text{for } \omega \in \mathbb{R},$$

cf. (3.8), and $\widehat{C}_Y(\omega)$ is assumed to be positive definite for $\omega \neq 0$. This shows that A is stable under the given assumption. \diamond

REMARK 3.5. A straightforward computation reveals that the inverse of the system matrix A , when in the block form representation given in (3.14), takes the form

$$A^{-1} = \begin{bmatrix} 0 & 0 & I \\ 0 & A^{-1} & A^{-1}C \\ -m\Omega_0^{-1} & m\Omega_0^{-1}B^T A^{-1} & m\Omega_0^{-1}B^T A^{-1}C \end{bmatrix}.$$

It follows that

$$A^{-1}E = \begin{bmatrix} 0 \\ 0 \\ -m\Omega_0^{-1} \end{bmatrix},$$

and hence,

$$E^T A^{-2}E = -m\Omega_0^{-1}.$$

On the other hand Proposition 3.3 implies that

$$\int_0^\infty t C_Y(t) dt = \int_0^\infty t E^T e^{tA} \Sigma_0 E dt = \frac{1}{\beta m} E^T \int_0^\infty t e^{tA} dt E,$$

and partial integration thus gives

$$\begin{aligned} \int_0^\infty t C_Y(t) dt &= \frac{1}{\beta m} E^T \left(t A^{-1} e^{tA} \Big|_{t=0}^\infty - \int_0^\infty A^{-1} e^{tA} dt \right) E \\ &= -\frac{1}{\beta m} E^T A^{-2} e^{tA} \Big|_{t=0}^\infty E = \frac{1}{\beta m} E^T A^{-2} E. \end{aligned}$$

We thus conclude that

$$\int_0^\infty t C_Y(t) dt = -\frac{1}{\beta} \Omega_0^{-1}.$$

Accordingly, compare (2.12), if C_Y is a good enough approximation of the true auto-correlation function C_V – in the sense that the first moment of C_Y (over the positive time axis) agrees well with the corresponding first moment of C_V – then Ω_0 is a good approximation of Ω .

Given the limited amount of data from which we start, this is not a foregone conclusion. On the other hand, if Ω is known beforehand then it is easy to incorporate this information into the construction of the Ornstein-Uhlenbeck system (3.2), namely by imposing

$$E^T A^{-2}E = -m\Omega^{-1} \tag{3.17}$$

as another constraint, so that Ω_0 and Ω coincide. \diamond

REMARK 3.6. Take note that C_{RV} is the antiderivative of C_V with $C_{RV}(0) = 0$ and C_R is the second antiderivative of $-C_V$ with $C_R(0) = (\beta\Omega)^{-1}$. Likewise, C_{XY} is the antiderivative of C_Y with $C_{XY}(0) = 0$ and C_X is the second antiderivative of $-C_Y$ with $C_X(0) = (\beta\Omega_0)^{-1}$. Accordingly, if we achieve a good match $C_Y \approx C_V$, then this will imply a good match of C_{XY} and C_{RV} and their counterparts C_{YX} and C_{VR} . And this then implies that C_X and C_R are also close to each other, provided that their initial values are in good agreement; otherwise we expect to see a systematic error in $C_R \approx C_X$ of size $\|\Omega^{-1} - \Omega_0^{-1}\|/\beta$. \diamond

4. Numerical construction of the Ornstein-Uhlenbeck process. We now present the numerical scheme that we use to generate the system (3.2) from given samples

$$c_\nu = C_V(\nu\tau), \quad \nu = 0, \dots, n,$$

for some $\tau > 0$ and $n \in \mathbb{N}$ of the true autocorrelation function C_V . As mentioned before, this algorithm is based on a method proposed in [5]; the differences are the particular side-constraints which are being used here (i) to cope for the external quadratic potential, and (ii) to provide additional safeguards to increase the success rate of the overall algorithm.

According to (3.6) the autocorrelation function of the Y -component of the stationary solution of (3.2) has the form

$$C_Y(t) = \frac{1}{\beta m} E^T e^{tA} E =: \frac{1}{\beta m} \varphi(t), \quad t \geq 0. \quad (4.1)$$

When A is diagonalizable with distinct eigenvalues $\lambda_1, \dots, \lambda_p \in \mathbb{C}^-$, its eigendecomposition gives the representation

$$A = \sum_{j=1}^p \lambda_j Q_j,$$

where $Q_j \in \mathbb{C}^{N \times N}$ are (oblique) projection matrices onto the associated eigenspaces; in our case, compare Section 4.3, this assumption on A is satisfied by construction, and each eigenspace has dimension d , generically. Using the above representation, φ can be written as a finite Prony series

$$\varphi(t) = \sum_{j=1}^p \Gamma_j e^{\lambda_j t}, \quad t \geq 0, \quad (4.2)$$

with coefficient matrices $\Gamma_j = E^T Q_j E \in \mathbb{C}^{d \times d}$; compare, e.g., Higham [15].

Since $\varphi(0) = I$ by virtue of (4.1) we conclude from (4.2) that

$$\sum_{j=1}^p \Gamma_j = I. \quad (4.3)$$

In addition, the constraints (3.7) and (3.17), which we want to impose on A , translate into further constraints on the coefficient matrices Γ_j in (4.2), namely

$$\sum_{j=1}^p \lambda_j \Gamma_j = 0 \quad \text{and} \quad \sum_{j=1}^p \lambda_j^{-1} \Gamma_j = 0, \quad (4.4)$$

respectively, and

$$\sum_{j=1}^p \lambda_j^{-2} \Gamma_j = -m \Omega^{-1}. \quad (4.5)$$

In view of (4.1) our goal now is to select a reasonable number $p \in \mathbb{N}$ of appropriate exponents $\lambda_j \in \mathbb{C}^-$ and associated coefficient matrices $\Gamma_j \in \mathbb{C}^{d \times d}$ such that φ provides a good match of our given data samples, i.e.,

$$\varphi(\nu\tau) = \sum_{j=1}^p \Gamma_j e^{\nu\tau\lambda_j} \approx \beta m c_\nu = \beta m C_V(\nu\tau) \quad (4.6)$$

for $\nu = 0, \dots, n$, while satisfying the constraints (4.3), (4.4) and – subject to the availability of Ω – (4.5).

4.1. Finding suitable exponents. To determine appropriate exponents λ_j we consider the generating function

$$F(z) = \sum_{\nu=0}^{\infty} c_{\nu} z^{-\nu-1} \quad (4.7)$$

of all equidistant snapshots c_{ν} of the underlying autocorrelation function C_V . This function is analytic in the exterior of the unit circle, because C_V is a bounded function, and hence the Laurent coefficients c_{ν} of F are also bounded. Let us assume for the moment that (4.6) holds true with equality for all $\nu \in \mathbb{N}_0$. Then we can insert this in (4.7) to obtain

$$\begin{aligned} F(z) &= \frac{1}{\beta m} \sum_{\nu=0}^{\infty} \sum_{j=1}^p \Gamma_j e^{\nu \tau \lambda_j} z^{-\nu-1} = \frac{1}{\beta m} \sum_{j=1}^p \frac{\Gamma_j}{z} \sum_{\nu=0}^{\infty} (e^{\tau \lambda_j} / z)^{\nu} \\ &= \frac{1}{\beta m} \sum_{j=1}^p \frac{\Gamma_j}{z - z_j} \end{aligned}$$

with

$$z_j = e^{\tau \lambda_j}, \quad j = 1, \dots, p.$$

Take note that this ansatz implies that F is a real rational function and that all the poles of F are inside the unit circle. We therefore proceed by approximating the generating function in the exterior of the unit disk by a rational function with the same two properties, using the AAA algorithm by Nakatsukasa, Sète, and Trefethen [23] for this purpose; more precisely, since F is matrix-valued, we use a matrix-valued variant of this algorithm which we borrow from Gosea and Güttel [8].

To be specific, let \mathcal{Z} be the set of all points of an equiangular grid with an even number of grid points on a circle $|\zeta| = \rho > 1$ in the complex plane, with the two real grid points at $\pm \rho$ as anchor points. The AAA algorithm determines a rational function in barycentric form

$$r(z) = \frac{\sum_{l=1}^p \frac{w_l F_l}{z - \zeta_l}}{\sum_{l=1}^p \frac{w_l}{z - \zeta_l}}, \quad (4.8)$$

where $\zeta_l \in \mathcal{Z}$ are the so-called support points, and w_l are suitable complex (scalar) weights. In the (generic) case that all weights are nonzero, the function (4.8) interpolates the given values $F_l \in \mathbb{C}^{d \times d}$ at all the support points, i.e.,

$$r(\zeta_l) = F_l, \quad l = 1, \dots, p.$$

Therefore, in order to approximate F of (4.7) we choose

$$F_l = \frac{1}{\beta m} \sum_{\nu=0}^n c_{\nu} \zeta_l^{-\nu-1} \approx F(\zeta_l) \quad \text{for } \zeta_l \in \mathcal{Z}, \quad (4.9)$$

and we mention that the quality of this approximation depends on the size of ρ and the corresponding truncation error on the one hand, and on the magnitude of any noise in the data on the other; ideally the choice of ρ is such that these two error components

balance each other; see [11] for a more detailed discussion of this matter. Note that $F_l = \overline{F_{l'}}$ when $\zeta_l = \overline{\zeta_{l'}}$, and hence, r is real, if the support points are real or come in complex conjugate pairs, and if the associated weights have the same property; we refer to [5, Appendix B.1] for a description how we determine appropriate weights with this property.

We initialize the list of support points with the two real grid points $\zeta_1 = \rho$ and $\zeta_2 = -\rho$, and then the AAA algorithm proceeds with a greedy iterative scheme: in the l -th iteration, $l = 1, 2, \dots$, two further grid points ζ_{2l+1} and $\zeta_{2l+2} = \overline{\zeta_{2l+1}}$ are added to the list of support points, where $\zeta_{2l+1} \in \mathcal{Z}$ is such that the Frobenius norm of the current residual $\|F_{2l+1} - r(\zeta_{2l+1})\|_F$ is maximal, unless the residual norms $\|F_i - r(\zeta_i)\|_F$ of all grid points $\zeta_i \in \mathcal{Z}$ are below a certain tolerance $\varepsilon > 0$ and a minimum number of admissible poles has been reached, in which case we stop the iteration. Note that the minimum number of admissible poles depends on the number of side constraints, see Proposition 4.1 below.

Once the iteration has been terminated we solve a generalized eigenproblem to compute the $p - 1$ poles of the rational approximation (4.8), cf. [23]. For every pole $z \neq 0$ with $|z| < 1$ the exponent(s)

$$\lambda = \begin{cases} \frac{1}{\tau} \log z, & z \notin \mathbb{R}^-, \\ \frac{1}{\tau} \log |z| \pm i \frac{\pi}{\tau}, & z \in \mathbb{R}^-, \end{cases} \quad |\operatorname{Im} \lambda| \leq \frac{\pi}{\tau}, \quad (4.10)$$

are used for the Prony series ansatz (4.2), while spurious poles outside the unit disk and in the origin are ignored, because they are caused by artefacts of the rational approximation. Since r is real, the resulting exponents are either real or come in complex conjugate pairs.

Take note that due to the definition (4.10) and due to spurious poles the value of p in (4.8) may slightly differ from the parameter p in (4.2), i.e., the number of terms of the Prony series. To enhance readability we nevertheless took the liberty to use the same letter here and there.

4.2. Finding suitable coefficient matrices. In a second step of our algorithm we determine coefficient matrices $\Gamma_j \in \mathbb{C}^{d \times d}$ for the Prony series φ of (4.2) by minimizing the data fit

$$\sum_{\nu=0}^n \|\varphi(\tau\nu) - \beta m c_\nu\|_F^2$$

in (4.6), subject to the aforementioned constraints (4.3) and (4.4), together with (4.5) in case the stiffness matrix Ω is to be incorporated.

In view of our ultimate goal (4.1) that φ coincides – up to the scalar factor βm – with the autocorrelation function of a stochastic process Y on the positive time axis, we have to make sure that φ , when extended by

$$\varphi(t) = \varphi(-t)^T, \quad t < 0, \quad (4.11)$$

to the negative time axis, is a function of positive type. A straightforward computation based on (4.2) shows that

$$\widehat{\varphi}(\omega) = \sum_{j=1}^p \left(\frac{\Gamma_j}{i\omega - \lambda_j} - \frac{\Gamma_j^T}{i\omega + \lambda_j} \right), \quad \omega \in \mathbb{R},$$

and hence, this expression has to be positive semidefinite for every $\omega \in \mathbb{R}$. In order to make this side condition numerically tractable we limit our attention to the (a priori known) zero eigenvalues of $\widehat{\varphi}$ at $\omega = 0$ and $\omega = \infty$. For high frequencies $\widehat{\varphi}(\omega)$ can be expanded into the convergent Laurent series

$$\widehat{\varphi}(\omega) = \sum_{k=0}^{\infty} \Upsilon_k \omega^{-k-1}$$

with selfadjoint coefficient matrices

$$\Upsilon_k = (-i)^{k+1} \sum_{j=1}^p \lambda_j^k \left(\Gamma_j + (-1)^{k+1} \Gamma_j^T \right), \quad k \in \mathbb{N}_0.$$

Accordingly, a necessary condition for $\widehat{\varphi}(\omega)$ to be positive semidefinite for large frequencies is that the first non-vanishing term of this Laurent series is positive semidefinite. Note that $\Upsilon_0 = \Upsilon_1 = 0$ according to (4.3) and (4.4), respectively. As a consequence, if Υ_2 happens to have a nonzero eigenvalue, then $\widehat{\varphi}(\omega)$ exhibits a negative eigenvalue when ω is large and has the appropriate sign. We therefore add the requirements that

$$\Upsilon_2/i = \sum_{j=1}^p \lambda_j^2 (\Gamma_j - \Gamma_j^T) = 0 \quad \text{and} \quad \Upsilon_3 = \sum_{j=1}^p \lambda_j^3 (\Gamma_j + \Gamma_j^T) \succcurlyeq 0$$

to our list of constraints.

Likewise, near the origin $\widehat{\varphi}(\omega)$ can be expanded into the Taylor series

$$\widehat{\varphi}(\omega) = \sum_{k=0}^{\infty} \Psi_k \omega^k$$

with

$$\Psi_k = -i^k \sum_{j=1}^p \lambda_j^{-k-1} \left(\Gamma_j + (-1)^k \Gamma_j^T \right), \quad k \in \mathbb{N}_0.$$

Here, $\Psi_0 = \Psi_1 = 0$ because of (4.4) and the fact that

$$\sum_{j=1}^p \Gamma_j \lambda_j^{-2} = \beta m \int_0^{\infty} t C_Y(t) dt = -m \Omega_0^{-1},$$

compare Remark 3.5, with Ω_0 being symmetric according to Proposition 3.3. We therefore impose the additional constraint that

$$\Psi_2 = \sum_{j=1}^p \lambda_j^{-3} (\Gamma_j + \Gamma_j^T) \succcurlyeq 0.$$

In summary, the optimization problem we consider takes the following form: Find coefficient matrices $\Gamma_j \in \mathbb{C}^{d \times d}$, $j = 1, \dots, p$, which minimize

$$\sum_{\nu=0}^n \left\| \sum_{j=1}^p \Gamma_j e^{\lambda_j \tau \nu} - \beta m c_{\nu} \right\|_F^2, \quad (4.12a)$$

subject to the equality constraints

$$\begin{aligned} \sum_{j=1}^p \Gamma_j &= I, & \sum_{j=1}^p \lambda_j \Gamma_j &= 0, \\ \sum_{j=1}^p \frac{1}{\lambda_j} \Gamma_j &= 0, & \sum_{j=1}^p \lambda_j^2 (\Gamma_j - \Gamma_j^T) &= 0, \end{aligned} \quad (4.12b)$$

the semidefiniteness constraints

$$\sum_{j=1}^p \lambda_j^3 (\Gamma_j + \Gamma_j^T) \succcurlyeq 0, \quad \sum_{j=1}^p \lambda_j^{-3} (\Gamma_j + \Gamma_j^T) \succcurlyeq 0, \quad (4.12c)$$

and the additional equality constraint

$$\sum_{j=1}^p \lambda_j^{-2} \Gamma_j = -\frac{1}{\beta} \Omega^{-1}, \quad \text{when } \Omega \text{ is prescribed.} \quad (4.12d)$$

PROPOSITION 4.1. *Assume that the number p of terms of the Prony series (4.2) satisfies $7 \leq p \leq n+1$. Then the optimization problem (4.12) has a solution $\{\Gamma_j\}_{j=1}^p \subset \mathbb{C}^{d \times d}$, and this solution gives rise to a real-valued Prony series (4.2). This solution is unique if the definition (4.10) of the exponents of the Prony series involves not more than one negative pole of the rational function. If there is more than one negative pole in (4.10) then there may be infinitely many real-valued Prony series (4.2) whose coefficient matrices solve the optimization problem (4.12); any two such solutions differ by a term of the form*

$$\psi(t) \sin(\pi t / \tau), \quad t \geq 0, \quad (4.13)$$

which vanishes at all grid points, where snapshots of C_V have been taken. The factor ψ in (4.13) is a linear combination of exponentials $e^{\mu_k t}$ with negative parameters μ_k and coefficient matrices in $\mathbb{R}^{d \times d}$.

Proof. The constraints (4.12b), (4.12c), and (4.12d) define a closed convex set \mathcal{C} . To see that \mathcal{C} is nonempty, consider the subset $\mathcal{C}_0 \subset \mathcal{C}$, which is obtained, when replacing the last constraint in (4.12b) and the two semidefiniteness constraints (4.12c) by the more restrictive equality constraints

$$\sum_{j=1}^p \lambda_j^2 \Gamma_j = 0, \quad \sum_{j=1}^p \lambda_j^3 \Gamma_j = 0, \quad \text{and} \quad \sum_{j=1}^p \lambda_j^{-3} \Gamma_j = 0.$$

The resulting seven constraints are inhomogeneous linear equality constraints of Vandermonde type, which have a solution, i.e., $\mathcal{C}_0 \neq \emptyset$, if the rectangular transposed Vandermonde matrix

$$\begin{bmatrix} 1 & \lambda_1 & \cdots & \lambda_1^6 \\ 1 & \lambda_2 & \cdots & \lambda_2^6 \\ \vdots & \vdots & & \vdots \\ 1 & \lambda_p & \cdots & \lambda_p^6 \end{bmatrix} \in \mathbb{C}^{p \times 7}$$

has a trivial null space, and this is the case whenever $p \geq 7$.

The objective function (4.12a) is convex on \mathcal{C} . Therefore the minimization problem (4.12) always has a solution if $p \geq 7$. Let $\{\Gamma_j\}$ be such a solution, and define another set of coefficient matrices $\{\tilde{\Gamma}_j\}$ via

$$\tilde{\Gamma}_j = \overline{\Gamma}_{j'}, \quad \text{where } \lambda_{j'} = \bar{\lambda}_j; \quad j = 1, \dots, p.$$

Then it is easy to see that $\{\tilde{\Gamma}_j\}$ also belongs to \mathcal{C} , and that the objective function attains the same minimal value for this second set of coefficient matrices. Due to convexity the same is true for the coefficient matrices $\{(\Gamma_j + \tilde{\Gamma}_j)/2\}$, for which the associated Prony series is real-valued.

Two different real-valued Prony series, whose coefficient matrices solve (4.12), must differ by a function which vanishes at all grid points $\nu\tau$, $\nu = 0, \dots, n$. Since $p \leq n + 1$ such a situation can only occur when some of the exponents of the two Prony series have an imaginary part $\pm\pi/\tau$; compare, for example, [25] in combination with [13, Remark 5.2]. According to (4.10) this (only) happens when the associated poles of the rational function are negative. This shows that if there are two Prony series φ_1 and φ_2 of this sort then $\varphi_2 - \varphi_1$ is a function of the form (4.13), where ψ is a linear combination of exponentials $e^{\mu_k t}$ and the exponents μ_k are the real parts of the corresponding exponents λ_k of the Prony series. From this it follows that

$$\varphi_2'(0) - \varphi_1'(0) = \frac{\pi}{\tau} \psi(0),$$

and hence, $\psi(0) = 0$ due to the second constraint in (4.12b). If there is only one negative pole then

$$\psi(t) = \psi(0)e^{\mu t}, \quad t \geq 0,$$

for some fixed value of μ , and therefore (4.13) vanishes identically, showing that the minimizer of (4.12) is unique in this case. \square

REMARK 4.2. The lower bound $p \geq 7$ is a conservative estimate of the necessary number of terms to guarantee feasibility of the list of constraints. For example, if $d = 1$ then the equality constraints in (4.12b) amount to three scalar equations in total, because the last one is always true; together with (4.12d) this gives four scalar equations, which can all be satisfied as soon as $p \geq 4$. For higher dimensions $p = 5$ terms of the Prony series are always sufficient to match all the equality constraints in (4.12b) and (4.12d), and it is conceivable that the semidefiniteness constraints in (4.12c) are also satisfied for the corresponding parameters. \diamond

In our code we solve (4.12) by first ignoring the semidefiniteness constraints (4.12c), and solving the resulting linearly constrained least-squares problem by classical linear algebra techniques, cf., e.g., Björck [4]. If the corresponding solution happens to satisfy (4.12c) then this is the solution of the full problem (4.12). Otherwise we add the constraints from (4.12c) which are violated by this approximation, and use a common technique to rewrite the resulting minimization problem as a semidefinite program, cf., e.g., Vandenberghe and Boyd [28]. Then we use the software package CVX [6, 9] to obtain a solution; CVX employs interior point methods for solving convex optimization problems. If the corresponding solution does still not satisfy (4.12c), we then solve the full problem (4.12) accordingly.

4.3. Construction of the Langevin system. In order to achieve the desired representation (4.1) for a particular function φ given by (4.2) we have to determine coefficient matrices A and L_0 of a suitable Langevin system (3.2).

For the construction of the (stable diagonalizable) drift matrix A we refer to the algorithm described in detail in [5, Appendix B.2]. The dimension of A is given by

$$N = \sum_{j=1}^p \text{rank}(\Gamma_j) \leq d \cdot p,$$

where the inequality arises because singular subspaces associated with any null space components of the coefficient matrices Γ_j are discarded. This is necessary to ensure that the realization (A, E, E) of the transfer function κ of (3.9) is minimal – using the language of system theory, cf. [2, Section 3.4]. In this case the Positive Real Lemma [2, Chapter 5] states that if and only if the transfer function is positive real, the (singular) Lur’e equations

$$AP + PA^T = -HH^T, \quad PE = E, \quad (4.14)$$

have real solution matrices P and H , where $P \in \mathbb{R}^{N \times N}$ is symmetric positive definite. On the other hand the transfer function is positive real, if and only if the extension (4.11) of φ is a function of positive type; compare (4.1) and (3.8). In other words, the Lur’e equations have a solution, if and only if the semidefiniteness constraints (4.12c), which we have imposed on the coefficients of φ , have been sufficient to determine an admissible Prony series approximation (4.2) of the given data. Moreover, cf. [2, Section 5.5], if this happens to be the case then there is a solution of (4.14) with $H \in \mathbb{R}^{N \times d}$, and due to the zero upper left block of A this matrix must have the form

$$H = \sqrt{\beta m} \begin{bmatrix} 0 \\ L_0 \end{bmatrix}$$

for some $L_0 \in \mathbb{R}^{(N-d) \times d}$. When this particular L_0 is used in (3.2), then $P/(\beta m)$ is the covariance matrix of the stationary solution of (3.2), and the autocorrelation function C_Y of the Y component of this solution coincides with $\varphi/\beta m$ as desired.

As shown in Section 3, a suitable variable transformation turns the matrix A into the equivalent form given in (3.1), and the stationary solution of (3.1) provides approximations of the velocity and the position of the macroparticle. Note that, as shown in Proposition 3.3, the Lur’e equations (4.14) are equivalent to the reduced Lur’e equations (3.15). Rather than (4.14) we therefore solve the latter ones for the remaining entry L of the fluctuating force term in (3.1), together with the covariance matrix Σ_{22} of the auxiliary variables Z .

The numerical solution of the singular Lur’e equations is rather involved and has been treated elsewhere. We refer to Wang, Speyer, and Weiss [29], for example; see also [5, Appendix C].

4.4. Position autocorrelation data. Finally, we briefly comment on the case that only position autocorrelation data

$$C_R(\nu\tau), \quad \nu = 0, \dots, n,$$

are given, in which case $\Omega = (\beta C_R(0))^{-1}$ is always known; compare Remark 2.2. As follows from the discussion in Remark 3.6, the autocorrelation functions C_Y and C_X of our searched-for Ornstein-Uhlenbeck process (3.1) satisfy

$$C_X''(t) = -C_Y(t). \quad (4.15)$$

Accordingly, if C_Y is given by (4.1), (4.2), with the constraints (4.3), (4.4), and (4.5) being satisfied, then

$$C_X(t) = -\frac{1}{\beta m} \sum_{j=1}^p \lambda_j^{-2} \Gamma_j e^{\lambda_j t}, \quad t \geq 0. \quad (4.16)$$

We therefore replace the generating function (4.7) by

$$F(z) = \sum_{\nu=0}^{\infty} C_R(\nu\tau) z^{-\nu-1},$$

use the AAA algorithm as described in Section 4.1 to determine a rational approximation of this function on a circle $|z| = \rho > 1$, and take its poles to define the exponentials of the Prony series (4.2); cf. (4.10).

In view of (4.16) we then determine the coefficients Γ_j in (4.2) as in Section 4.2, replacing the objective function (4.12a) by

$$\sum_{\nu=0}^n \left\| \sum_{j=1}^p \lambda_j^{-2} \Gamma_j e^{\lambda_j \tau \nu} + \beta m C_R(\tau \nu) \right\|_F^2.$$

Beware of the fact that the two terms in the norm are now coupled with a plus sign because of the minus sign in (4.16). Further note, that while the stiffness matrix Ω is readily available in this case, the mass matrix is not and therefore has to be provided as additional information.

A potential advantage of using position data is that in some applications position data decay more slowly than velocity data and therefore provide a better signal to noise ratio; on the other hand, high frequency information in the velocity data is damped in the position autocorrelation function by virtue of (4.15).

5. Numerical results.

Example 5.1. As our first example we consider the translation and rotation invariant system of a spherical particle in a harmonic trap, which gives rise to one-dimensional processes V and R . The detailed setup of this system and the generation of corresponding molecular dynamics data for the four cross-correlation functions C_V , C_R , C_{VR} , and C_{RV} is specified in Appendix A. These four scalar functions are shown as black dashed lines in Figure 5.1.

We now discuss constructions $X \approx R$ and $Y \approx V$ computed by the algorithms proposed above. For our first two algorithms we use $n+1 = 41$ samples of the velocity autocorrelation function with a grid spacing $\tau = 0.025$ as input; the corresponding grid therefore covers the initial time interval $[0, 1]$. These first two algorithms differ in that the first one assumes that Ω is known a priori, so we enforce the constraint (4.12d) for this approximation, while the second one assumes that Ω is unknown. Accordingly, the resulting two approximations C_Y of C_V use the same number of terms in the Prony series (4.2) and the same exponents, because the latter are determined in the first phase of our algorithm, which is the same for both methods. In this first phase, where we employ the AAA algorithm, cf. Section 4.1, we evaluate the generating function on an equiangular grid with 100 grid points on a circle with radius $\rho = 1.15$. After initializing the list of support points with the two real grid points at $\pm\rho$, the AAA algorithm performs three iterations in this example and determines a rational function

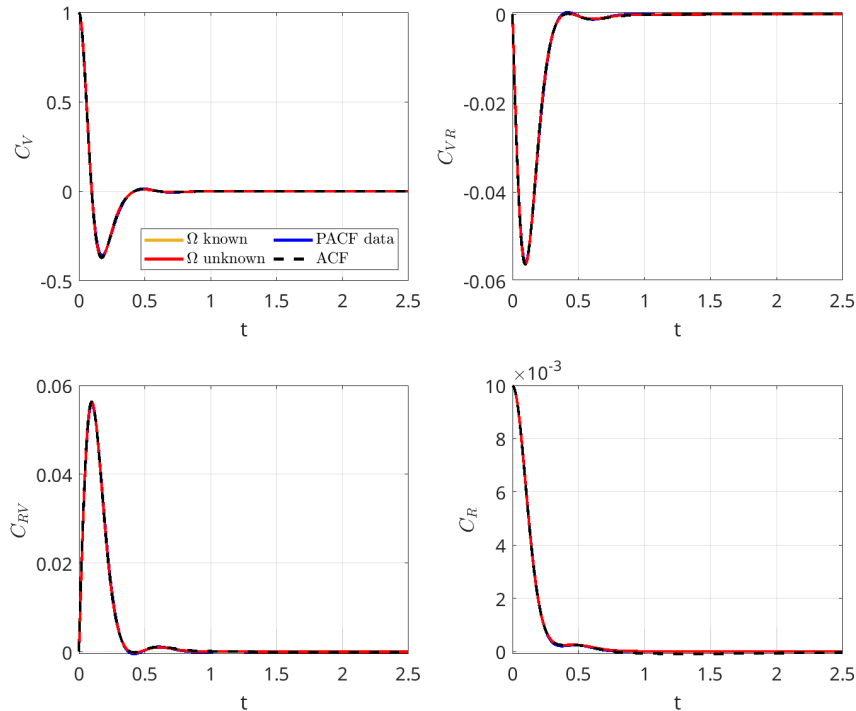


FIG. 5.1. Autocorrelation function of Example 5.1 versus time t and the three numerical approximations. Each panel shows the scalar graphs corresponding to the respective entry of the matrix-valued function.

with seven admissible poles to reduce the residuals below the tolerance $\varepsilon = 10^{-4}$. One of these poles is positive, and the remaining ones come in three complex conjugate pairs. The two resulting Prony series approximations of the velocity autocorrelation function thus have $p = 7$ terms, each.

We determine the (scalar) coefficients Γ_j of these Prony series as described in Section 4.2. Recall from Proposition 4.1 that the associated constrained least-squares problems (4.12) have unique solutions, each, and note that according to Remark 4.2 we have seven free parameters to satisfy three or four scalar equations in the present one-dimensional case, depending on whether (4.12d) is included as a constraint or not. The remaining degrees of freedom provide the flexibility to optimize the least-squares fit. In either case, i.e., with and without the constraint (4.12d), the solution of the linearly constrained linear least squares problems is no feasible solution of the full convex problem (4.12), because \mathcal{Y}_3 happens to be negative. Therefore the semidefinite program is invoked to solve the optimization problem; since Ψ_2 has been positive in this example we only add the constraint $\mathcal{Y}_3 \geq 0$ to the previous equality constraints. In both cases the software CVX returns an approximate solution of (4.12) which is feasible in that both, \mathcal{Y}_3 and Ψ_2 , are positive. Also, the singular Lur'e equations (4.14) turn out to be solvable in both cases, so the two Prony series approximations yield valid autocorrelation functions. The resulting two Ornstein-Uhlenbeck systems have dimension $N = d \cdot p = 7$, each, and therefore they come with $7 - 2 = 5$ auxiliary

variables.

The third algorithm uses samples of the position autocorrelation function instead of velocity data; compare Section 4.4. These data are sampled on a grid with the same grid spacing $\tau = 0.025$ as before, but this time we only use $n + 1 = 31$ data points corresponding to the time interval $[0, 0.75]$. The reason is – as can be seen from Figure 5.2 (see the text below) – that the autocorrelation function reaches the noise level near $t = 0.75$ while the velocity autocorrelation function stays above the noise level for all $t \in [0, 1]$. Accordingly, we also choose a larger value $\rho = 1.2$ for computing interpolation data (4.9) for the generating function to achieve a similar (relative) truncation level as before despite the reduced number of available terms in (4.9). Here we run the AAA algorithm with the smaller stopping tolerance $\varepsilon = 10^{-6}$ to cope for the fact that $C_R(0) = (\beta\Omega)^{-1} = 1/100$ is two orders of magnitude smaller than the sample values of the velocity autocorrelation function that have been used above. The AAA algorithm performs two iterations and returns a rational function with five admissible poles, one of them being positive and the remaining four being complex conjugate pairs. So the resulting Prony series approximation of C_V has $p = 5$ terms. It turns out that the solution of the corresponding linearly constrained linear least squares problem is feasible in that \mathcal{T}_3 and Ψ_2 are both positive. The solution of the corresponding Lur'e equations yields an Ornstein-Uhlenbeck process of dimension $N = d \cdot p = 5$, which means that the corresponding system has three auxiliary variables.

The associated autocorrelation functions are depicted in Figure 5.1: The orange graphs correspond to the functions where velocity autocorrelation data and the value of Ω are being used, the red graphs correspond to velocity autocorrelation data without the use of Ω , and the blue ones are the approximations based on position autocorrelation data. In these plots the blue and orange lines are almost fully covered by the red ones, which in turn show a very good alignment with the original data (in black). For a better evaluation of the quality of these approximations we refer to Figure 5.2, which shows the absolute differences between the respective approximation and the true values in a semilogarithmic scale; also included here are the reference functions (in black); otherwise, the color coding is the same as in Figure 5.1. Returning to what we have indicated before, the black lines decay down to an absolute noise level of about 10^{-4} ; for the velocity autocorrelation function (top left panel) this is reached near $t = 1.5$, whereas the position autocorrelation function (bottom right panel) is down to the noise level already at about $t = 0.75$. Since the Prony series decay exponentially their errors are dominated by the reference function values, as soon as the latter have reached the noise level. One can further see that the two approximations from velocity data are significantly better than the third one in blue by almost one order of magnitude. This reflects the situation that more samples of the velocity data could be used, which led to more terms in the corresponding Prony series and thus to a better data fit; compare the final remark in Section 4.4. The two approximations based on velocity autocorrelations in turn have fairly similar quality; only in an initial time interval the match of the position autocorrelation data differs because of the slight misfit of the Ω -approximation: the corresponding estimate $C_X(0) = (\beta\Omega_0)^{-1}$ can be seen to differ from the true value $C_R(0) = 0.01$ by a relative error of 10^{-3} , roughly, which is similar to the errors in the approximations of C_V . But aside of that, in this example the incorporation of the additional constraint (4.12d) does not lead to a significant benefit.

As in [5] we have varied the number of grid points to test the robustness of our

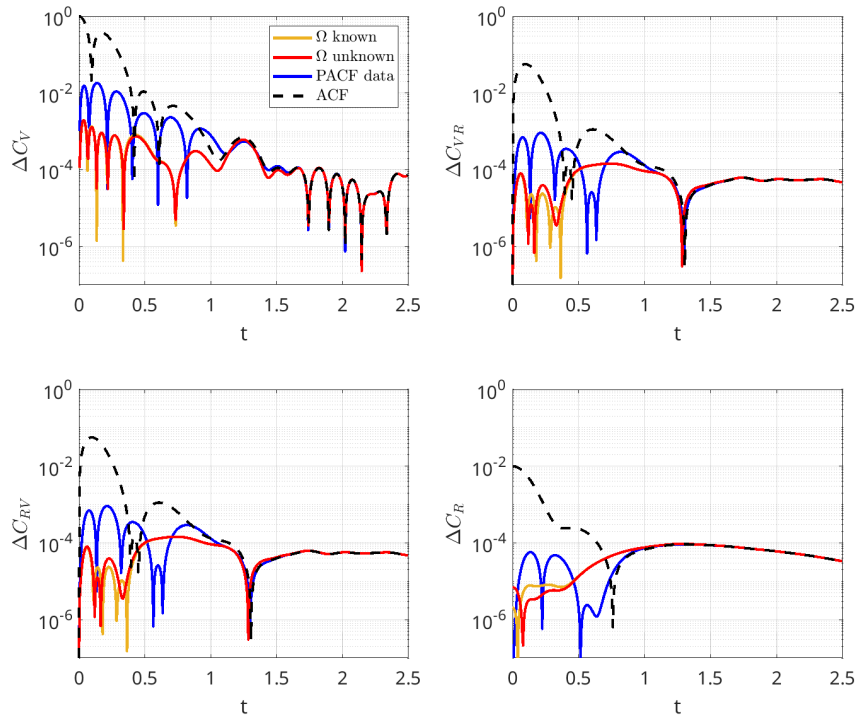


FIG. 5.2. Absolute error between the true autocorrelation function of Example 5.1 and the three approximations. Each panel contains the scalar graphs corresponding to the error of the respective entry of the matrix-valued approximation. The black dashed lines show the target functions for additional information.

algorithm. Note that our algorithm is not fail-proof in that we only incorporate a necessary condition for our approximation φ to be of positive type; compare Section 4.2. If φ fails to be of positive type then the Lur'e equations have no solution, and we cannot generate a corresponding Ornstein-Uhlenbeck process. It turns out that for this example, the robustness of the method is very similar to the one in [5]: our algorithm has been successful for the vast majority of tests that we have made.

Example 5.2. Next we consider the dynamics of two coupled particles of different masses in a harmonic trap, which gives rise to two-dimensional processes V and R , each. Again we refer to Appendix A for a detailed description of the physical system. In this example we focus on the use of velocity data, which are displayed in Figure 5.3, because the numerical results for position data have been inferior in Example 5.1. More precisely, we use $n + 1 = 31$ samples of $C_V \in \mathbb{R}^{2 \times 2}$ with a grid spacing of $\tau = 0.1$ as input data, covering the initial time interval $[0, 3]$; as can be seen from the insets in Figure 5.3, near $t = 4$ the individual entries of C_V reach the absolute noise level of about $5 \cdot 10^{-4}$.

This time we need to preprocess the given data, because the mass matrix is not a multiple of the identity matrix, compare (2.1). To this end we rescale the velocity autocorrelation function C_V by computing the Cholesky decomposition $C_V(0) = L_C L_C^T$

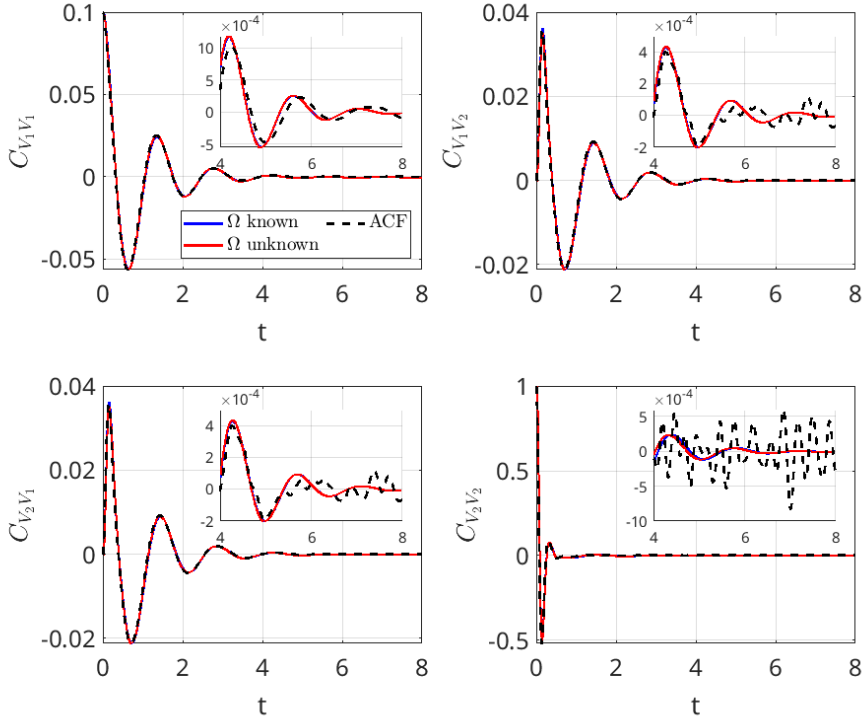


FIG. 5.3. Velocity autocorrelation function of Example 5.2 versus time and the two approximations with and without the integral constraint (4.12d). Each panel shows the scalar graphs corresponding to the respective entry of the matrix-valued function.

and multiplying $C_V(t)$ by L_C^{-1} and L_C^{-T} from left and right, respectively. After preprocessing the data, the corresponding generating function is evaluated for the AAA scheme on an equiangular grid with 100 grid points on a circle, this time with radius $\rho = 1.5$. The AAA algorithm performs four iterations to reduce the residuals below the error tolerance of $\varepsilon = 5 \cdot 10^{-4}$, and provides a matrix-valued rational function with seven admissible poles. One of these poles is negative and is thus duplicated according to (4.10); the other six poles consist of two real and two complex conjugate pairs. The Prony series ansatz thus has $p = 8$ terms in this particular example.

Take note here that since we only have one negative pole and $p \geq 7$, the optimization problem (4.12) for the coefficient matrices of the Prony series has a unique minimizer according to Proposition 4.1. Again we compute two approximations, one with and one without the integral constraint (4.12d). In both cases the solution of the linearly constrained linear least squares problem is not in the feasible set of the overall convex optimization problem, because \mathcal{T}_3 fails to be positive definite; We add the violated constraint to the list of constraints and use CVX for the solution of the augmented optimization problems. This leads to a feasible approximate minimizer in the case of using (4.12d), but fails in the second case. The reason is that now \mathcal{T}_3 is positive definite as requested, but Ψ_2 is not. We therefore restart CVX for this instance with both semidefiniteness constraints and finally obtain feasible approximate minimizers of (4.12) for both cases. The corresponding singular Lur'e equations

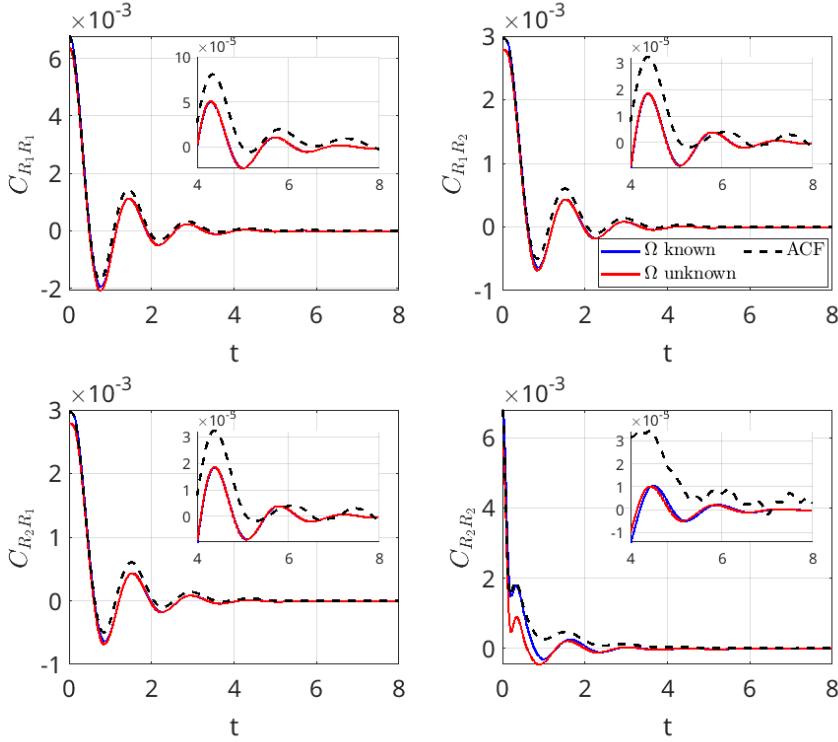


FIG. 5.4. Position autocorrelation function of Example 5.2 versus time and the two approximations with and without the integral constraint (4.12d). Each panel shows the scalar graphs corresponding to the respective entries of the matrix-valued function.

(4.14) are solvable, and therefore the two Prony series approximations provide valid autocorrelation functions $C_Y \approx C_V$. The resulting Ornstein-Uhlenbeck system has dimension $N = d \cdot p = 16$, which corresponds to $16 - 4 = 12$ auxiliary variables.

See Figure 5.3 for a plot of C_V and the two approximations C_Y and Figure 5.4 for the corresponding position autocorrelation functions. Here the blue lines correspond to the functions where Ω is known and the red lines correspond to the other ones, respectively, and the reference functions are black and dashed. It can be seen that the velocity autocorrelation functions provide an excellent match for both algorithms, while the approximations of the position autocorrelation functions are slightly inferior. We omit plots of the cross-correlations; the fits are of comparable quality.

Concerning the use of the Ω -constraint (4.12d) one can only see a benefit in the lower right panel of Figure 5.4; otherwise the two approximations are of very similar quality. This is also confirmed in Figure 5.5, which provides a better quantitative picture of the error of the respective approximations. In this figure we display the Frobenius norm of the errors in the 2×2 correlation functions C_V , C_R , and C_{RV} versus time. Here the left-hand panel corresponds to the approximation where Ω is prescribed, whereas the right-hand panel corresponds to the approximation which presumes Ω to be unknown. We observe similar error histories in both panels; only for $t < 1$ the error in C_R is better in the left panel, where Ω has been prescribed. Overall, the absolute error in C_R is smaller by about one order of magnitude, but the

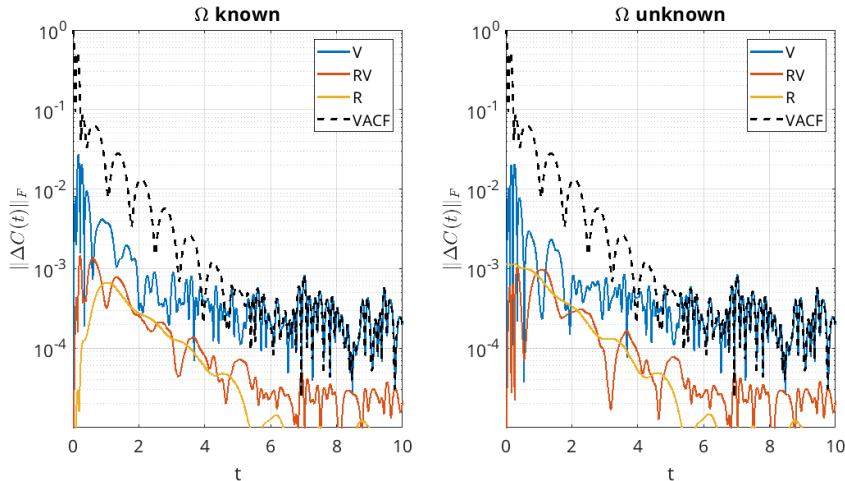


FIG. 5.5. Absolute error between the given velocity, position and cross correlation of Example 5.2 and the two approximations. The left panel shows the approximation error where Ω is known, the right panel where Ω is unknown, respectively.

individual entries of C_R in itself are also smaller than those of C_V by (at least) the same amount.

6. Conclusion. In this work we have presented a framework for constructing Markovian embeddings for generalized (multidimensional) Langevin equations with an external harmonic potential from autocorrelation data. We have further discussed conditions for stationary solutions of these equations. The algorithm which we suggest is an extension of a method presented in [5] to cope for the harmonic potential in the system. This method determines a rational approximation with a matrix-valued version of the AAA algorithm of the generating function of the given data and uses the poles of this rational function to choose the exponential terms of a Prony series approximation of the data. The coefficients of this expansion are determined by solving a linear least-squares problem with semidefiniteness constraints. Numerical experiments with one- and two-dimensional molecular dynamics data have been shown to be very successful and indicate that the method has a high potential to generalize faithfully to more complex physical data.

Appendix A. Details of the molecular dynamics simulation. The test data for the two examples in Section 5 have been generated with the software package LAMMPS [26] (stable release April 2, 2025). To be specific we have simulated a liquid of 1000 particles interacting with a Weeks-Chandler-Andersen potential [30] using the TVN-ensemble, where the mass of the particles, the thermal energy, and the characteristic energy and length scale parameters of the interaction potential are unity in the reduced unit system. The cubic simulation box with periodic boundary conditions has an edge length of 10.7722 spatial units corresponding to a particle density of 0.8. The initial configuration, with all particles on a regular Cartesian grid with unit grid spacing, has been set up using the molecular builder Moltemplate [16].

For the one dimensional system discussed in Example 5.1 one of the particles (our particle of interest) is attached to its starting position by a harmonic spring with spring constant $\Omega = 100$. To remove the linear momentum introduced into the liquid

by this external force the center of mass motion of the liquid is set to zero every 1000 steps. Using a timestep of 0.005 we integrate both systems for $5 \cdot 10^4$ steps with a Langevin thermostat (cf., e.g., Dünweg and Paul [7]) using a thermostat constant of one time unit to obtain equilibrated structures. Then, to obtain 50 independent configurations of each system we randomize the velocity of all particles and integrate for another 10^5 steps with a Nosé-Hoover-type thermostat (Tuckerman et al [27]) using a thermostat constant of 5.0 time units. Finally we integrate these 50 independent systems for 10^7 steps, each, saving the position and velocity of the trapped particles at every time step. The correlation functions are averaged over all 50 systems and all three spatial dimensions.

For the two dimensional system we use the same setting, except that we set the time step to 0.0025 and attach two neighboring particles to their starting positions with harmonic springs with spring constant $\Omega = 100$, each, and on top of that, connect these two particles with an elastic rod with spring constant $\Omega = 50$. We modify the mass of the second particle to be $m = 10$, i.e., ten times heavier than the first one, and we switch off the Weeks-Chandler-Andersen interaction between the two particles. Finally, we constrain two coordinates of the two particles to their initial values and only allow their motion in the third coordinate axis of the Cartesian grid; accordingly the velocities of the two tagged particles are scalar functions, each. Take note that in this example so-called depletion layers around the two particles under consideration give rise to additional external forces acting on these particles, cf., e.g., Lekkerkerker, Tuinier, and Vis [20], and therefore the quadratic form (1.3) of the potential Φ is just its leading order approximation.

REFERENCES

1. L.V. AHLFORS, *Complex Analysis*, 3rd ed., McGraw-Hill, Inc., New York, 1979.
2. B.D.O. ANDERSON AND S. VONGPANITLERD, *Network Analysis and Synthesis: A Modern Systems Theory Approach*, Prentice-Hall, Englewood-Cliffs, NJ, 1973.
3. A.D. BACZEWSKI AND S.D. BOND, Numerical integration of the extended variable generalized Langevin equation with a positive Prony representable memory kernel, *J. Chem. Phys.* **139** (2013), 044107.
4. Å. BJÖRCK, *Numerical Methods for Least Squares Problems*, 2nd ed., SIAM, Philadelphia, 2024.
5. N. BOCKIUS, M. BRAUN, K. HOFMANN, F. SCHMID, AND M. HANKE, Determining extended Markov parameterizations for vector-valued generalized Langevin equations, *Z. Naturforschung A* **81** (2026), 157–171.
6. CVX RESEARCH INC., CVX: Matlab software for disciplined convex programming, version 2.0. <http://cvxr.com/cvx>, 2011.
7. B. DÜNWEG AND W. PAUL, Brownian dynamics simulations without Gaussian random numbers, *Int. J. Mod. Phys. C* **2** (1991), 817–827.
8. I.V. GOSEA AND S. GÜTTEL, Algorithms for the Rational Approximation of Matrix-Valued Functions, *SIAM J. Sci. Comput.* **43** (2021), A3033–A3054.
9. M.C. GRANT AND S.P. BOYD, Graph implementations for nonsmooth convex programs, in *Recent Advances in Learning and Control*, V.D. Blondel, S.P. Boyd and H. Kimura (eds), Lecture Notes in Control and Information Sciences, Vol. 371, Springer, London, 2008, pp. 95–110.
10. G. GRIPENBERG, S.-O. LONDEN AND O. STAFFANS, *Volterra Integral and Functional Equations*, Cambridge University Press, Cambridge, 1990.
11. R. GRIESMAIER AND M. HANKE, One shot inverse scattering revisited, *SIAM J. Imaging Sci.* **18** (2025), 881–905.
12. F. GROGAN, H. LEI, X. LI, AND N.A. BAKER, Data-driven molecular modeling with the generalized Langevin equation, *J. Comp. Phys.* **418** (2020), 109633.
13. M. HANKE, Stochastic modeling of stationary scalar Gaussian processes in continuous time from autocorrelation data, *Adv. Comput. Math.* **50** (2024), 60.
14. M. HANKE, The second fluctuation-dissipation theorem for the generalized Langevin equation,

- manuscript, arXiv:2507.17350 (2025).
15. N.J. HIGHAM, *Functions of Matrices: Theory and Computation*, SIAM, Philadelphia, 2008.
 16. A.I. JEWETT, D. STELTER, J. LAMBERT, S.M. SALADI, O.M. ROSCIONI, M. RICCI, L. AUTIN, M. MARITAN, S.M. BASHUSQEH, T. KEYES, R.T. DAME, J.-E. SHEA, G.J. JENSEN, AND D.S. GOODSSELL, Moltemplate: A tool for coarse-grained modeling of complex biological matter and soft condensed matter physics, *J. Mol. Biol.* **11** (2021), 166841.
 17. V. KLIPPENSTEIN, N. WOLF, AND N.F.A. VAN DER VEGT, A Gauss-Newton method for iterative optimization of memory kernels for generalized Langevin thermostats in coarse-grained molecular dynamics simulations, *J. Chem. Phys.* **160** (2024), 204115.
 18. B. KOWALIK, J.O. DALDROP, J. KAPPLER, J.C.F. SCHULZ, A. SCHLAICH, AND R.R. NETZ, Memory-kernel extraction for different molecular solutes in solvents of varying viscosity in confinement, *Phys. Rev. E* **100** (2019), 012126.
 19. H. LEI, N.A. BAKER, AND X. LI, Data-driven parameterization of the generalized Langevin equation, *Proc. Nat. Acad. Sci. U.S.A.* **113** (2016), 14183–14188.
 20. H.N.W. LEKKERKERKER, R. TUINIER, AND M. VIS, *Colloids and the Depletion Interaction*, 2nd ed., Springer, Cham, 2024.
 21. G. LINDGREN, *Stationary Stochastic Processes. Theory and Applications*, CRC Press, Boca Raton, 2013.
 22. L. MA, X. LI, AND C. LIU, The derivation and approximation of coarse-grained dynamics from Langevin dynamics, *J. Chem. Phys.* **145** (2016), 204117.
 23. Y. NAKATSUKASA, O. SÈTE, AND L.N. TREFETHEN, The AAA algorithm for rational approximation, *SIAM J. Sci. Comput.* **40** (2018), A1494–A1522.
 24. G.A. PAVLIOTIS, *Stochastic Processes and Applications. Diffusion Processes, the Fokker-Planck and Langevin Equations*, Springer, New York, 2014.
 25. G. PLONKA, D. POTTS, G. STEIDL, AND M. TASCHE, *Numerical Fourier Analysis*, Springer, Cham, 2018.
 26. A.P. THOMPSON, H.M. AKTULGA, R. BERGER, D.S. BOLINTINEANU, W.M. BROWN, P.S. CROZIER, P.J. IN 'T VELD, A. KOHLMAYER, S.G. MOORE, T.D. NGUYEN, R. SHAN, M.J. STEVENS, J. TRANCHIDA, C. TROTT, AND S.J. PLIMPTON, LAMMPS – a flexible simulation tool for particle-based materials modeling at the atomic, meso, and continuum scales, *Comput. Phys. Commun.* **271** (2022), 108171.
 27. M.E. TUCKERMAN, J. ALEJANDRE, R. LÓPEZ-RENDÓN, A.L. JOCHIM, AND G.J. MARTYNA, A Liouville-operator derived measure-preserving integrator for molecular dynamics simulations in the isothermal-isobaric ensemble, *J. Phys. A* **19** (2006), 5629.
 28. L. VANDENBERGHE AND S. BOYD, Semidefinite Programming, *SIAM Review* **38** (1996), 49–95.
 29. Q. WANG, J. SPEYER AND H. WEISS, System characterization of positive real conditions, in *29th IEEE conference on Decision and Control, Honolulu, USA*, IEEE, 1990, pp. 348–353.
 30. J.D. WEEKS, D. CHANDLER, AND H.C. ANDERSEN, Role of repulsive forces in determining the equilibrium structure of simple liquids, *J. Chem. Phys.* **54** (1971), 5237–5247
 31. R. ZWANZIG, *Nonequilibrium Statistical Mechanics*, Oxford University Press, Oxford, 2001.